

First order metamagnetic transition in $\text{Ho}_2\text{Ti}_2\text{O}_7$ observed by vibrating coil magnetometry at milli-Kelvin temperatures

C. Krey,¹ S. Legl,¹ S. R. Dunsiger,¹ M. Meven,² J. S. Gardner,³ J. M. Roper,⁴ and C. Pfleiderer¹

¹*Technische Universität München, Physik-Department E21, D-85748 Garching, Germany*

²*Technische Universität München, Forschungsneutronenquelle FRM II, D-85748 Garching, Germany*

³*Department of Physics, Indiana University, Bloomington, IN 47408, USA*

⁴*Los Alamos National Laboratory, Los Alamos, USA*

(Dated: November 8, 2018)

We report vibrating coil magnetometry of the spin ice system $\text{Ho}_2\text{Ti}_2\text{O}_7$ down to ~ 0.04 K for magnetic fields up to 5 T applied parallel to the [111] axis. History dependent behavior emerges below $T_0^* \sim 0.6$ K near zero magnetic field, in common with other spin ice compounds. In large magnetic fields we observe a magnetization plateau followed by a hysteretic metamagnetic transition. The temperature dependence of the coercive fields as well as the susceptibility calculated from the magnetization identify the metamagnetic transition as a line of first order transitions terminating in a critical endpoint at $T_m^* \simeq 0.37$ K, $B_m \simeq 1.5$ T. The metamagnetic transition in $\text{Ho}_2\text{Ti}_2\text{O}_7$ is strongly reminiscent of that observed in $\text{Dy}_2\text{Ti}_2\text{O}_7$, suggestive of a general feature of the spin ices.

PACS numbers: 75.30.Kz; 75.60.Ej; 75.40.Cx; 75.40.Gb

Metamagnetism (MMT), where a paramagnet undergoes a first order phase transition to a ferromagnetic (FM) state in high magnetic fields with a discontinuous jump in the magnetisation, is a pervasive phenomenon in systems based on rare earth or transition metals. However, despite striking similarities in the magnetization of a wide range of MMTs their microscopic origin may be radically different (see e.g. [1–6]). A prominent example of such a MMT has been reported recently for $\text{Dy}_2\text{Ti}_2\text{O}_7$, where the transition is preceded by a plateau in the magnetization and a critical end-point is located at $T_m \sim 0.36$ K and $B_m \sim 0.9$ T for fields strictly parallel to a $\langle 111 \rangle$ axis [7, 8]. It has been argued that the MMT in $\text{Dy}_2\text{Ti}_2\text{O}_7$ reflects directly the nature of the spin excitations from the zero-field spin state [9]. The magnetic ions in $\text{Dy}_2\text{Ti}_2\text{O}_7$ reside on the vertices of a pyrochlore lattice of corner sharing tetrahedra in the presence of strong local $\langle 111 \rangle$ crystalline anisotropy and effective ferromagnetic interactions, leading to geometric frustration. The ground state is characterized by a residual entropy quantitatively comparable to the value of water ice [10–12]. This reflects spin disorder at low temperature such that two spins are constrained to point outward and two spins in towards the center of a tetrahedron [11, 13].

The MMT in $\text{Dy}_2\text{Ti}_2\text{O}_7$ has been explained in terms of an entropy reduction which takes place in two steps [14]. First, the system partially magnetises retaining the two-in, two-out state, in which one of the four spins on each tetrahedron has a component of the moment antiparallel to the field. Second, as the field increases further, the nearest-neighbor spin ice model predicts an ice-rule breaking spin flip to the three-in, one-out (one-in, three out) state [15, 16]. Recent theoretical work suggests that the spin-flips related to the second step may be viewed as emergent magnetic monopoles that condense at the MMT [9, 17]. This scenario was subsequently found to

be consistent with the entropy reduction inferred from the magnetocaloric effect [8, 18], as well as the evolution of the spin relaxation time in the ac susceptibility [19, 20], at least above 1 K. The strong temperature dependence of the specific heat below 1 K [21], the heat transport [22] and finally magnetization avalanches in low magnetic fields [23] are also thought to be consistent with magnetic monopoles. On a microscopic level, evidence for magnetic monopoles in $\text{Dy}_2\text{Ti}_2\text{O}_7$ has been inferred from the observation of lines of reversed spins between monopole pairs (cf. Dirac strings) using neutron scattering [21].

A second candidate for emergent magnetic monopoles is $\text{Ho}_2\text{Ti}_2\text{O}_7$. The experimental situation in $\text{Ho}_2\text{Ti}_2\text{O}_7$ is, however, much less clear. Neutron scattering at low temperatures reveals pinch-points in the structure factor consistent with power law correlation functions [24, 25]. However, neutron spin echo and neutron backscattering experiments [26–28] suggest intrinsic spin relaxation times much faster than for $\text{Dy}_2\text{Ti}_2\text{O}_7$, raising the question how this may be reconciled in terms of magnetic monopoles. Further, the specific heat displays large nuclear hyperfine contributions [29], which manifest themselves as a Schottky anomaly, complicating a comparison with the predictions for spin ice behaviour. The magnetization of $\text{Ho}_2\text{Ti}_2\text{O}_7$ for a field along [111] reported so far down to 0.5 K [30, 31] showed a non-linear increase around 2 T reminiscent of $\text{Dy}_2\text{Ti}_2\text{O}_7$ (distinct from discussions of a liquid-gas transition for fields along [100] [32]). In general, the magnetic phase diagram of Ho-based compounds may show strong effects below 0.5 K due to hyperfine interactions as e.g., for the transverse field Ising magnet LiHoF_4 [33]. Hence, detailed measurements well below 0.5 K are needed to explore the putative equivalence between $\text{Ho}_2\text{Ti}_2\text{O}_7$ and $\text{Dy}_2\text{Ti}_2\text{O}_7$ quantitatively.

The observation of history dependencies and dynamics on long timescales in $\text{Dy}_2\text{Ti}_2\text{O}_7$ and $\text{Ho}_2\text{Ti}_2\text{O}_7$ in previous studies imposes strong experimental constraints. First, tiny sample movements in the applied magnetic field must be avoided; they might change the magnetic state. Second, the sample must be rigidly anchored thermally, since changes of the magnetization may cause large associated entropy release and uncontrolled local heating effects. Third, as the magnetic properties are sensitive to the precise field value and orientation [34, 35] a uniform applied field is essential.

All of these requirements are met by the vibrating coil magnetometer (VCM) [36, 37] we used to measure the magnetization of $\text{Ho}_2\text{Ti}_2\text{O}_7$. Data reported in the following between 0.04 K and ~ 1.8 K correspond to the properties for field parallel to [111] within a few tenths of a degree. For larger misalignments ($\sim \pm 2^\circ$) we found that the features of interest tend to broaden and shift, with additional hysteretic features suggesting complexities beyond the scope of our study. All temperature dependent data were recorded while continuously heating at a rate of 5 mK/min, where zero-field cooled properties and field-cooled properties are distinguished. Likewise, all measurements as a function of magnetic field followed one of two well defined protocols, denoted as (A) and (B). Details of the temperature dependent measurements as well as the two protocols are presented in the supplementary material.

The $\text{Ho}_2\text{Ti}_2\text{O}_7$ single crystal studied was grown by means of optical float zoning at LANL in an argon atmosphere at 5 mm/hr. Single crystal neutron diffraction at HEIDI (FRM II) establish a room temperature lattice constant of $a=10.13(2)$ Å consistent with previous studies [38]. A psi scan of the (555) reflection confirms the homogeneity and high quality of the sample. Demagnetising fields were accounted for by approximating the disc shaped single crystal as an ellipsoid ($7.3 \times 4.8 \times 1.2$ mm³) with a demagnetising factor $N=0.75$ ([111] direction perpendicular to the plane) [39, 40]. The edges of the sample were wedge shaped, which may result in a distribution of internal fields over a small volume fraction. This does not affect the main conclusions reported here.

Shown in Fig. 1 (a) is the temperature dependence of the magnetization of $\text{Ho}_2\text{Ti}_2\text{O}_7$ for $B = 0.01$ T along [111]. With decreasing temperature the low-field magnetization increases gradually, characteristic of a paramagnetic state. Below a temperature $T_0^* \sim 0.6$ K the zfc/fh and fc/fh data begin to show pronounced differences. While the former rapidly decreases to a very low value, the latter remain constant. This behaviour is strongly reminiscent of other spin ices, where T_0^* is roughly 0.6-0.75 K for $\text{A}_2\text{B}_2\text{O}_7$ ($\text{A}=\text{Dy},\text{Ho}$; $\text{B}=\text{Ti}, \text{Sn}$) [30, 41, 42], i.e., T_0^* is *not* proportional to the rare earth exchange coupling J [43]. The microscopic origin of the history dependence shares many features of magnetic blocking, but is not understood. For instance, Monte Carlo simu-

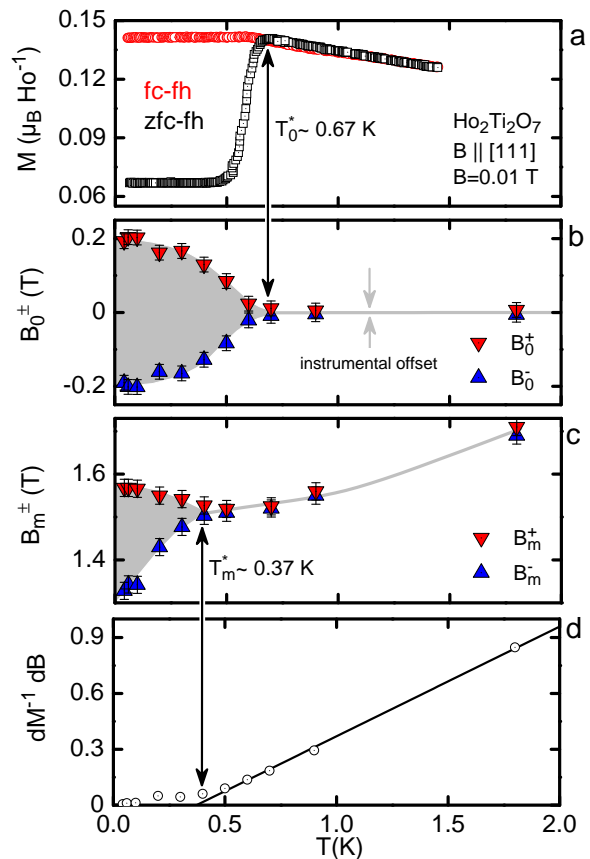


FIG. 1: (Color online) Characteristic features of the magnetization of spin freezing, hysteresis and a metamagnetic transition ending in a critical point in $\text{Ho}_2\text{Ti}_2\text{O}_7$. (a) Temperature dependence of the magnetization of $\text{Ho}_2\text{Ti}_2\text{O}_7$ for [111] in a small applied field of 0.01 T. (b) Temperature dependence of the coercive fields with respect to zero field. (c) Temperature dependence of the coercive fields at the metamagnetic transition. (d) Temperature dependence of the peak value of the inverse susceptibility with decreasing temperature, approaching the metamagnetic transition.

lations predict a 1st order transition at 0.18K [44] which has never been observed experimentally. Interestingly, however, an exponential slowing down of the spin relaxation has been reported in solid paramagnets which proceeds via energy levels caused by crystalline or hyperfine splitting of the ground state of the ion [45].

As a function of magnetic field the history dependence below T_0^* is connected with strong hysteresis with respect to $B = 0$, followed by a metamagnetic increase at a field $B_m^\pm \sim 1.5$ T, which becomes distinctly hysteretic at low temperatures. This is illustrated in Fig. 2, where typical data are shown as a function of *internal* magnetic field, B_{int} , given by $\mu_0 H + M$. Data at 1.8 K shown in Fig. 2 (a) are in excellent agreement with Refs. [30, 31]. The variation of the magnetization near $B = 0$ and around 1.5 T becomes much steeper below $T_0^* = 0.7$ K as shown in

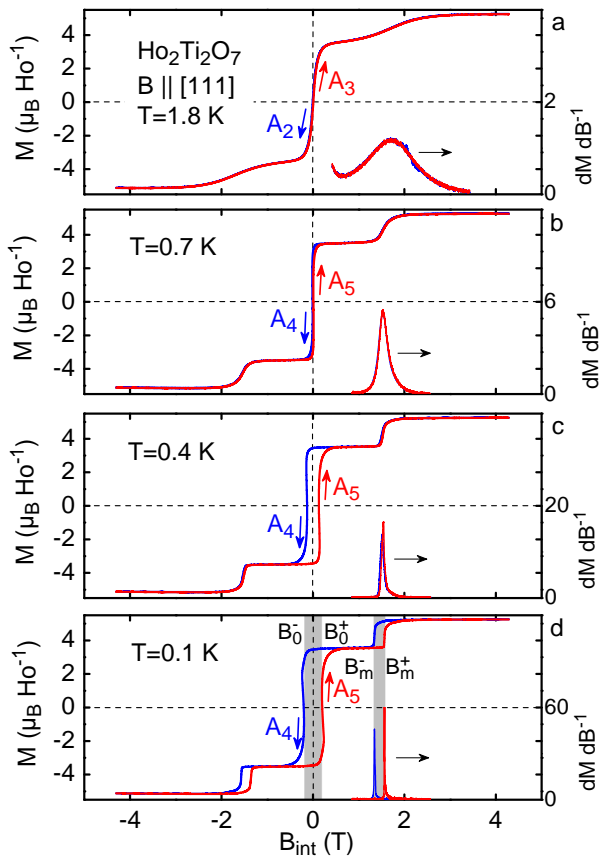


FIG. 2: (Color online) Magnetic field dependence of the low temperature magnetization of $\text{Ho}_2\text{Ti}_2\text{O}_7$. With decreasing temperature, hysteresis emerges at $B = 0$ and around 1.5 T. The susceptibility calculated from the magnetization is shown on the right hand side of each panel. At the metamagnetic transition it increases strongly with decreasing temperature.

Fig. 2 (b). There are several regimes: essentially no hysteresis is observed at 0.7 K within the accuracy of our set-up. At $T = 0.4 \text{ K} < T_0^*$, shown in Fig. 2 (c), sizeable hysteresis may be seen with respect to zero field, while the magnetization at the second step rises non-hysteretically, but more steeply than at 0.7 K. Finally, as shown in Fig. 2 (d), hysteresis exists with respect to both $B = 0$ and $B_m = 1.5 \text{ T}$ for 0.1 K.

In order to track the width of the hysteresis loop we define coercive fields B_0^-, B_0^+ and B_m^-, B_m^+ (see Fig. 2 (d)). Shown in Fig. 1 (b) are the coercive fields B_0^-, B_0^+ , which increase strongly below T_0^* with decreasing temperature and appear to level off around $\pm 0.2 \text{ T}$ as $T \rightarrow 0$. In contrast, the hysteretic behaviour at high fields appears at $T_m^* = 0.37 \text{ K}$, well below T_0^* (Fig. 1(c)).

No conventional long range thermodynamic ordering transition is reported as a function of temperature at $B = 0$, despite the appearance of strong hysteresis. Specifically, there is no development of magnetic Bragg peaks. Rather, the notion of strong magnetic blocking is beautifully illustrated by the initial field dependence

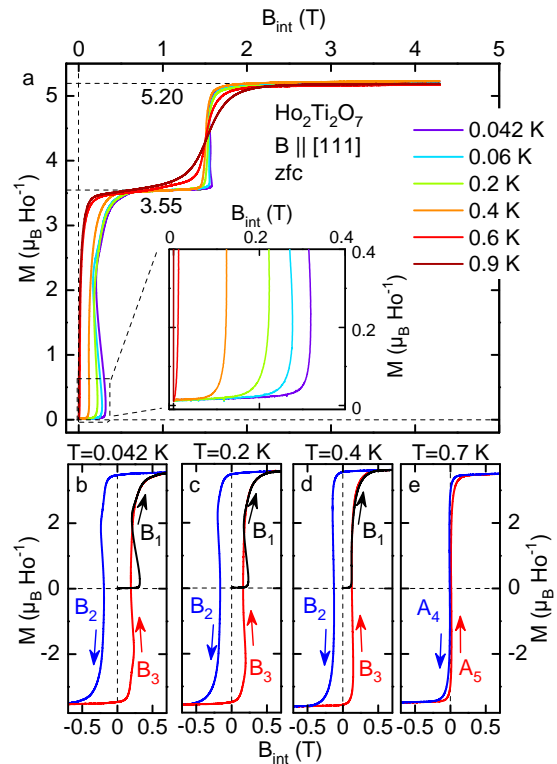


FIG. 3: (Color online) magnetization of $\text{Ho}_2\text{Ti}_2\text{O}_7$ as a function of internal magnetic field after correction of the demagnetising fields, following field sweeps of protocol (B). For $T < T_0^*$ the initial change of the magnetization is zero within experimental sensitivity and followed by a very pronounced increase with increasing field. (a) Magnetic field dependence in sweeps of type B1. (b) through (d) magnetization in field cycles of sweep types B1, B2 and B3 (e) magnetization in field cycles of sweep types A4 and A5.

of the magnetization for $T < T_0^*$ after zfc. Shown in Fig. 3 (a) is the magnetization in the first field sweep after zero-field cooling (referred to as B1). Up to field values exceeding the coercive fields seen in field sweeps (B2), (B3) the magnetization is unchanged and trapped in the zfc state. The peculiar field dependence, specifically the negative slope of the magnetization at intermediate fields is reminiscent of $\text{Dy}_2\text{Ti}_2\text{O}_7$ (Fig. 3 (b) through (e)), where it has been interpreted as evidence of monopole avalanches [23]. However, similar features have also been reported in mesoscopic spin systems [46]. In view of the enormous sensitivity to the precise orientation of the sample and the large demagnetising factor, as well as a small distribution of internal fields at its fringes, a detailed account of possible magnetization avalanches is beyond the scope of our study.

Two arguments establish that the hysteresis at B_m is connected with a thermodynamic phase transition, in contrast to the behaviour in zero field. First, the inverse susceptibility at B_m calculated from the magneti-

zation essentially displays a Curie dependence and vanishes within experimental accuracy at $T_m^* = 0.37(0.01)$ K and $B_m^* = 1.52(0.01)$ T as shown in Fig. 1 (d). This is characteristic of a critical point at (T_m^*, B_m^*) . Moreover, the hysteresis observed for $T < T_m^*$ provides evidence that this critical point is located at the end of a line of first order transitions. Interestingly, T_m^* is found to be very close to the value for $\text{Dy}_2\text{Ti}_2\text{O}_7$ [7]. By contrast, theory predicts scaling of B_m^* with the effective exchange coupling J_{eff} [18, 47]. Given $J_{\text{eff}} = 5D/3 + J/3$, where D is the dipolar coupling between the rare earth moments, and using $J_{\text{eff}}/k_B = 1.1$ K for $\text{Dy}_2\text{Ti}_2\text{O}_7$ and 1.83 K for $\text{Ho}_2\text{Ti}_2\text{O}_7$ [11], the phase boundary for the latter is predicted to occur at 1.49 T. The agreement between theory and experiment is very satisfying.

Second, following the Clausius-Clapeyron equation (CC), $dB_m/dT = -\Delta S/\Delta M$, the transition at B_m is connected with a strong entropy reduction of a thermodynamic phase transition subject to the value of dB_m/dT . Because the transition at B_m is hysteretic determination of the phase boundary using CC depends on the choice of dB_m/dT . As a first step it is instructive to suppose Kagomé ice behaviour for $B < B_m$. In this case a rigorous calculation predicts an entropy reduction of $0.672^{-1} \text{ mol}^{-1}\text{-ion}$ [48]. The corresponding value of $dB_m/dT = 0.073$ T/K, as shown by the solid black line passing through (T_m^*, B_m^*) in Fig. 4 is perfectly consistent with our data and follows the cross-over line for $T > T_m^*$. However, the phase boundary would lie asymmetrically with respect to B_m^+ and B_m^- . If we assume instead that B_m is located midway in the hysteretic field range or at the field of the peak of dM/dB we find $dB_m/dT \approx 0.2$ T/K. In this case the expected entropy release at B_m exceeds the entropy associated with Kagomé ice by an unphysically large factor of 3.65. Hence the latter prescription must be inappropriate.

Strong support for the assumption of Kagomé ice behaviour for $B < B_m$ may be seen in the magnetization, which forms a very well defined plateau at $3.55 \mu_B \text{ Ho}^{-1}$ (cf Fig. 3 (a)). This is quantitatively in excellent agreement with theoretical prediction. Moreover, above B_m the magnetization assumes a well-defined value of $5.20 \mu_B \text{ Ho}^{-1}$ for $T \rightarrow 0$ characteristic of a three-in/one-out spin configuration. Thus the magnetization of $\text{Ho}_2\text{Ti}_2\text{O}_7$ is quantitatively comparable with that of $\text{Dy}_2\text{Ti}_2\text{O}_7$ and consistent with the dipolar spin ice model. The temperature dependence of B_m^+ and B_m^- and the magnetization provide unambiguous evidence of a first order transition with a large entropy reduction. Experimental determinations of the residual entropy of the Kagomé ice state inferred from the specific heat in $\text{Dy}_2\text{Ti}_2\text{O}_7$ for $B < B_m$ are scattered between $0.44(8) - 0.8(1) \text{ J K}^{-1} \text{ mol}^{-1}\text{-Dy}$ [16, 49], consistent with the value inferred from the magnetization, $0.5 \text{ J K}^{-1} \text{ mol}^{-1}\text{-Dy}$ [7]. The temperature dependence of the entropy release in the magnetocaloric effect in $\text{Dy}_2\text{Ti}_2\text{O}_7$ [8] is attributed

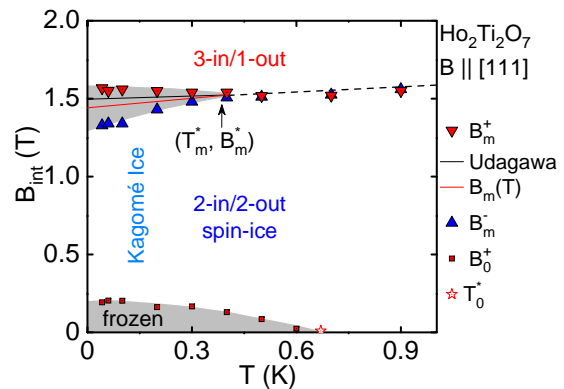


FIG. 4: (Color online) Magnetic phase diagram of $\text{Ho}_2\text{Ti}_2\text{O}_7$ for magnetic field parallel to [111]. With respect to $B = 0$ strong freezing and hysteresis emerges in the magnetization below $T_0^* = 0.67$ K in the presence of the residual dynamics seen microscopically [26–28]. At high fields a line of first order metamagnetic transitions terminates in a critical endpoint. The metamagnetic transition separates Kagomé ice behaviour from a three-in/one-out configuration when going from below to above B_m .

to magnetic correlations [50].

We finally show in Fig. 4 the magnetic phase diagram of $\text{Ho}_2\text{Ti}_2\text{O}_7$ for the [111] axis inferred from our magnetization data. In zero field $\text{Ho}_2\text{Ti}_2\text{O}_7$ enters a spin ice state with strong spin blocking below T_0^* . A moderate field stabilises a magnetization plateau characteristic of Kagomé ice. Further increasing the field results in a line of first order metamagnetic phase transitions up to a critical endpoint at $T_m^* = 0.37$ K and $B_m^* = 1.52$ T. This line of transitions separates Kagomé ice from the spin polarised 3-in/1-out configuration. While the critical field for $T \rightarrow 0$ scales experimentally with the J_{eff} , in agreement with theory, T_0^* and T_m^* appear to be material independent for $\text{Ho}_2\text{Ti}_2\text{O}_7$ and $\text{Dy}_2\text{Ti}_2\text{O}_7$. The tuning parameter for these energy scales remains to be explored.

In conclusion, the remarkable analogy we observe between the properties of $\text{Dy}_2\text{Ti}_2\text{O}_7$ and $\text{Ho}_2\text{Ti}_2\text{O}_7$ establishes the field induced liquid-gas like transition, interpreted in terms of the condensation of magnetic monopoles, as a more generic phenomenon within spin ice systems. However, given the importance of dipolar interactions and the resultant power law correlations [25] as an essential prerequisite for a description of the excitations in terms of magnetic monopoles, it also seems clear that further Ising like compounds *not* based on Ho or Dy, which have similar classical magnetic moments, must be investigated. In this way, the strength of the dipolar coupling could be controllably tuned. Perhaps most remarkably, the phase boundaries appear to be independent of the strength of the hyperfine interactions, which are much stronger in $\text{Ho}_2\text{Ti}_2\text{O}_7$. It is important to note that the dc magnetization is a measure of the *zero*

frequency response of the system. Subleading transverse interactions J_{\pm} which are material dependent and could lead for instance to differing quantum tunnelling amplitudes between spin-ice states are predicted to affect the *finite* frequency response [51]. A complete description of the excitations in terms of magnetic monopoles must account for such differences.

We wish to thank P. Böni, R. Moessner, R. Ritz, A. Regnat and C. Franz for support and stimulating discussions. Financial support through DFG TRR80 and DFG FOR960 are gratefully acknowledged. CK acknowledges support through the TUM Graduate School.

-
- [1] P. Haen, J. Flouquet, F. Lapiere, P. Lejay, and G. Remenyi, *Journal of Low Temperature Physics* **67**, 391 (1987).
- [2] C. Thessieu, C. Pfleiderer, A. N. Stepanov, and J. Flouquet, *Journal of Physics: Condensed Matter* **9**, 6677 (1997).
- [3] M. Uhlarz, C. Pfleiderer, and S. M. Hayden, *Phys. Rev. Lett.* **93**, 256404 (2004).
- [4] R. S. Perry, L. M. Galvin, S. A. Grigera, L. Capogna, A. J. Schofield, A. P. Mackenzie, M. Chiao, S. R. Julian, S. I. Ikeda, S. Nakatsuji, et al., *Phys. Rev. Lett.* **86**, 2661 (2001).
- [5] M. Iijima, K. Endo, and T. Sakakibara, *Journal of Physics: Condensed Matter* **2**, 10069 (1990).
- [6] T. Goto, K. Fukamichi, and H. Yamada, *Physica B: Condensed Matter* **300**, 167 (2001).
- [7] T. Sakakibara, T. Tayama, Z. Hiroi, K. Matsuhira, and S. Takagi, *Phys. Rev. Lett.* **90**, 207205 (2003).
- [8] H. Aoki, T. Sakakibara, K. Matsuhira, and Z. Hiroi, *Journal of the Physical Society of Japan* **73**, 2851 (2004).
- [9] C. Castelnovo, R. Moessner, and S. L. Sondhi, *Nature* **451**, 42 (2008).
- [10] A. P. Ramirez, A. Hayashi, R. J. Cava, R. Siddharthan, and B. S. Shastry, *Nature* **399**, 333 (1999).
- [11] S. T. Bramwell and M. J. P. Gingras, *Science* **294**, 1495 (2001).
- [12] M. J. P. Gingras, *Introduction to Frustrated Magnetism* (Springer-Verlag, Berlin, 2011).
- [13] M. J. Harris, S. T. Bramwell, M. D. F., T. Zeiske, and K. W. Godfrey, *Phys. Rev. Lett.* **79**, 2554 (1997).
- [14] S. V. Isakov, K. S. Raman, R. Moessner, and S. L. Sondhi, *Phys. Rev. B* **70**, 104418 (2004).
- [15] H. Fukazawa, R. G. Melko, R. Higashinaka, Y. Maeno, and M. J. P. Gingras, *Phys. Rev. B* **65**, 054410 (2002).
- [16] K. Matsuhira, Z. Hiroi, T. Tayama, S. Takagi, and T. Sakakibara, *Journal of Physics: Condensed Matter* **14**, L559 (2002).
- [17] I. Ryzhkin, *Journal of Experimental and Theoretical Physics* **101**, 481 (2005).
- [18] Z. Hiroi, K. Matsuhira, S. Takagi, T. Tayama, and T. Sakakibara, *Journal of the Physical Society of Japan* **72**, 411 (2003).
- [19] J. Snyder, B. G. Ueland, J. S. Slusky, H. Karunadasa, R. J. Cava, A. Mizel, and P. Schiffer, *Phys. Rev. Lett.* **91**, 107201 (2003).
- [20] L. D. C. Jaubert and P. C. W. Holdsworth, *Nature Physics* **5**, 258 (2009).
- [21] D. J. P. Morris, D. A. Tennant, S. A. Grigera, B. Klemke, C. Castelnovo, R. Moessner, C. Czternasty, M. Meissner, K. C. Rule, J. Hoffmann, et al., *Science* **326**, 411 (2009).
- [22] B. Klemke, M. Meissner, P. Strehlow, K. Kiefer, S. Grigera, and D. Tennant, *Journal of Low Temperature Physics* **163**, 345 (2011).
- [23] D. Slobinsky, C. Castelnovo, R. A. Borzi, A. S. Gibbs, A. P. Mackenzie, R. Moessner, and S. A. Grigera, *Phys. Rev. Lett.* **105**, 267205 (2010).
- [24] T. Fennell, P. P. Deen, A. R. Wildes, K. Schmalzl, D. Prabhakaran, A. T. Boothroyd, R. J. Aldus, D. F. McMorrow, and S. T. Bramwell, *Science* **326**, 415 (2009).
- [25] C. L. Henley, *Annu. Rev. Condens. Matter Phys.* **1**, 179 (2010).
- [26] G. Ehlers, A. L. Cornelius, M. Orendac, M. Kajnakova, T. Fennell, S. T. Bramwell, and J. S. Gardner, *Journal of Physics: Condensed Matter* **15**, L9 (2003).
- [27] G. Ehlers, A. L. Cornelius, T. Fennell, M. Koza, S. T. Bramwell, and J. S. Gardner, *Journal of Physics: Condensed Matter* **16**, S635 (2004).
- [28] J. P. Clancy, J. P. C. Ruff, S. R. Dunsiger, Y. Zhao, H. A. Dabkowska, J. S. Gardner, Y. Qiu, J. R. D. Copley, T. Jenkins, and B. D. Gaulin, *Phys. Rev. B* **79**, 014408 (2009).
- [29] S. T. Bramwell, M. J. Harris, B. C. den Hertog, M. J. P. Gingras, J. S. Gardner, D. F. McMorrow, A. R. Wildes, A. L. Cornelius, J. D. M. Champion, R. G. Melko, et al., *Phys. Rev. Lett.* **87**, 047205 (2001).
- [30] O. A. Petrenko, M. R. Lees, and G. Balakrishnan, *Journal of Physics: Condensed Matter* **23**, 164218 (2011).
- [31] O. A. Petrenko, M. R. Lees, and G. Balakrishnan, *Phys. Rev. B* **68**, 012406 (2003).
- [32] M. J. Harris, S. T. Bramwell, P. C. W. Holdsworth, and J. D. M. Champion, *Phys. Rev. Lett.* **81**, 4496 (1998).
- [33] M. Schechter and P. C. E. Stamp, *Phys. Rev. B* **78**, 054438 (2008).
- [34] H. Sato, K. Matsuhira, T. Tayama, Z. Hiroi, S. Takagi, and T. Sakakibara, *Journal of Physics: Condensed Matter* **18**, L297 (2006).
- [35] H. Sato, K. Matsuhira, T. Sakakibara, T. Tayama, Z. Hiroi, and S. Takagi, *Journal of Physics: Condensed Matter* **19**, 145272 (2007).
- [36] S. Legl, Ph.D. thesis, Technische Universität München, Physik Department E21 (2010).
- [37] S. Legl, C. Pfleiderer, and K. Krämer, *Review of Scientific Instruments* **81**, 043911 (2010).
- [38] M. Subramanian, G. Aravamudan, and G. S. Rao, *Progress in Solid State Chemistry* **15**, 55 (1983).
- [39] J. A. Osborn, *Phys. Rev.* **67**, 351 (1945).
- [40] J. A. Quilliam, L. R. Yaraskavitch, H. A. Dabkowska, B. D. Gaulin, and J. B. Kycia, *Phys. Rev. B* **83**, 094424 (2011).
- [41] K. Matsuhira, Y. Hinatsu, K. Tenya, and T. Sakakibara, *Journal of Physics: Condensed Matter* **12**, L649 (2000).
- [42] J. Snyder, B. G. Ueland, J. S. Slusky, H. Karunadasa, R. J. Cava, and P. Schiffer, *Phys. Rev. B* **69**, 064414 (2004).
- [43] B. C. den Hertog and M. J. P. Gingras, *Phys. Rev. Lett.* **84**, 3430 (2000).
- [44] R. G. Melko, B. C. den Hertog, and M. J. P. Gingras, *Phys. Rev. Lett.* **87**, 067203 (2001).
- [45] V. A. Atsarkin, *Physics Letters A* **130**, 492 (1988).
- [46] C. Paulsen and J.-G. Park, *Quantum Tunneling of Mag-*

netization - QTM94 (Kluwer, Dordrecht, Netherlands, 1995).

- [47] R. Moessner and S. L. Sondhi, Phys. Rev. B **68**, 064411 (2003).
- [48] M. Udagawa, M. Ogata, and Z. Hiroi, Journal of the Physical Society of Japan **71**, 2365 (2002).
- [49] R. Higashinaka, H. Fukazawa, and Y. Maeno, Phys. Rev. B **68**, 014415 (2003).
- [50] Y. Tabata, H. Kadowaki, K. Matsuhira, Z. Hiroi, N. Aso, E. Ressouche, and B. Fåk, Phys. Rev. Lett. **97**, 257205 (2006).
- [51] O. Benton, O. Sikora, and N. Shannon, arXiv:1204.1325, (2012).

**SUPPLEMENTARY MATERIAL FOR: FIRST
ORDER METAMAGNETIC TRANSITION IN
HO₂TI₂O₇ OBSERVED BY VIBRATING COIL
MAGNETOMETRY AT MILLI-KELVIN
TEMPERATURES**

In this supplement we present a detailed account of the precise temperature and field history used in our measurements and the terminology used to refer to specific temperature and field sweeps in the main text.

Temperature dependence

We distinguish two types of temperature sweeps, namely zero-field cooled/field heated (zfc/fh) and field-cooled/field heated (fc/fh). In both cases data were recorded while heating the sample continuously at a rate of 5 mK/min. Data denoted as zfc/fh were recorded after initially cooling the superconducting magnet system and cryostat from room temperature, to guarantee the absence of any remanent magnetic fields. To record data denoted as fc/fh, we re-cooled the sample to base temperature after the zfc/fh measurement was completed (at roughly 1.5 K), keeping the magnetic field unchanged. Data were then recorded again while continuously heating.

Field dependence: Protocol A

For field sweeps following protocol (A) the empty VCM was at first demagnetised and the sample cooled in zero magnetic field to $T = 1.8$ K. Data were subsequently recorded in three field sweeps as follows: (A1) $0 \rightarrow +5$ T, (A2) $+5$ T $\rightarrow -5$ T, and (A3) -5 T $\rightarrow +5$ T. At the final field of $+5$ T the temperature was changed. At each subsequent temperature two field sweeps were carried out, namely (A4) $+5$ T $\rightarrow -5$ T and (A5) -5 T $\rightarrow +5$ T.

At temperatures above 0.1 K all data were recorded while sweeping the field continuously at 15 mT/min. Below 0.1 K, to avoid heating effects due to eddy currents, data were recorded in a step mode, holding the magnetic field constant while recording the magnetisation.

Field dependence: Protocol B

For measurements following protocol (B) the empty VCM was at first demagnetised and the sample subsequently cooled in zero magnetic field from room temperature directly to the temperature of interest. Data were then recorded in a sequence of three field sweeps: (B1) $0 \rightarrow +5$ T, (B2) $+5$ T $\rightarrow -5$ T, and (B3) -5 T $\rightarrow +5$ T. For the next set of measurements following protocol (B) the sample was removed from the VCM and the empty VCM again demagnetised.

At temperature below 0.1 K and for all sweeps of type (B1) data were recorded in a step mode. All other data were recorded while sweeping the field continuously at 15 mT/min. No differences were observed between (A4), (A5) and (B2), (B3), respectively.

	sweep #	field values	condition
protocol (A)	A1	$0 \text{ T} \rightarrow 5 \text{ T}$	zfc to 1.8 K
	A2	$+5 \text{ T} \rightarrow -5 \text{ T}$	
	A3	$-5 \text{ T} \rightarrow +5 \text{ T}$	
	A4	$+5 \text{ T} \rightarrow -5 \text{ T}$	field-cooled
	A5	$-5 \text{ T} \rightarrow +5 \text{ T}$	field-cooled
protocol (B)	B1	$0 \text{ T} \rightarrow +5 \text{ T}$	zfc from ambient
	B2	$+5 \text{ T} \rightarrow -5 \text{ T}$	
	B3	$-5 \text{ T} \rightarrow +5 \text{ T}$	

TABLE I: Summary of protocol (A) and (B) used in measurements as a function of magnetic field. Zero-field-cooled and field-cooled starting conditions are denoted as zfc and fc, respectively.